Effect of Molecular Orientation on Polymer Free Volume Distribution: An Atomistic Approach

Hai Dong and Karl I. Jacob*

Polymer Education & Research Center, School of Polymer, Textile and Fiber Engineering, Georgia Institute of Technology, Atlanta, Georgia 30332-0295

Received June 4, 2003; Revised Manuscript Received September 3, 2003

ABSTRACT: Many mechanical and rheological properties of polymers are related to the amount and the distribution of its free volume. In this work, the evolution of free volume and its distribution in a linear model polymer resembling polyethylene under extensional strain are studied using a combination of molecular dynamics (MD) and Voronoi tessellation. When the molecular orientation due to stretch increases, the total number of voids in the sample decreases along with the number-average void size, while the number of larger unoccupied regions in the polymer increases, which become more elongated due to stretch. The hand-sphere probe shows that the overall free volume is decreasing during stretching; however, the reduction is not distributed evenly in the region. Free volume associated with atoms located away from the ends of molecular chains decreases while the free volume associated with atoms located at the molecular ends increases with stretch. Results from this computational work are in good agreement with several experimental observations reported in the literature.

Introduction

The concept of free volume has long been used to interpret and explain phenomena such as the glass transition, chain dynamics, physical aging, and transport behavior in polymeric systems.[1−3] Although the total free volume offers a quantitative description, the distribution of free volume is also considered to govern the underlying physics.[4] Consequently, there have recently been some efforts to determine the free volume distribution by experimental techniques, utilizing for example positron annihilation lifetime (PAL) spectroscopy[5] and the kinetics of isomerization of probe molecules added to glassy polymers.[6,7] These experimental techniques are sometimes laborious and involve some ambiguities in interpreting the results quantitatively in terms of free volume distribution. Computer modeling of polymer materials provides an alternative method of evaluating free volume distribution under a variety of conditions perhaps with less ambiguity.[4] The methods of molecular dynamics (MD) coupled with a relatively unambiguous way of evaluating the unoccupied space existing between polymer atoms offer a methodology to calculate the free volume and its distribution in a polymer under increasing strains. The shape and size evolution of these voids could be followed in time for polymer systems subjected to time-dependent changes.

In this work, two techniques were applied to characterize the free volume distribution for a model polymer undergoing increasing uniaxial strains. First, the hard-sphere probe method divides the periodic box into small cubic cells with a grid size that depends on the distribution of interatomic separation distance, but usually less than 1 Å.[8−10] Each grid was then tested to find whether it is occupied or not. Connectivity of voids was formed when two unoccupied subcells share a common face. All the unoccupied subcells having connectivity were assigned to the same void. The system then can be characterized by the distribution of void volume and shape. The shape of a void is often evaluated by reduced dimensionless surface-to-volume ratio, the shape factor w, defined by

$$w = (S/4\pi)/(3V/4\pi)^{2/3} \quad (1)$$

where S and V refer to the cavity surface area and volume, respectively. The parameter has a minimum value of 1.0 for a sphere.

Although not a direct measure of free volume in the strict sense, a number of researchers have attempted to use the distribution of Voronoi polyhedron volumes as an indicator of relative "free" volume distributions within various materials. Voronoi tessellation has been adopted by several researchers to study the geometry of systems with computer simulations.[4,11,12] It divides the system into convex polyhedra that surround each atom, as shown in Figure 1.[13] A larger polyhedron volume around one atom indicates larger free volume around that atom.

It is known that a denser packing of amorphous polymer resulting from drawing or stretching reduces its fractional free volume. The consequence of this behavior is lowering of diffusivity and gas permeability.[14−16] The recent experimental data from Shelby et al., however, suggested chain alignment causes an increase in the number of larger, more elliptical free volume holes in amorphous polymers, while the polymer density increases with stretching.[17,18] In the present study, we applied MD simulations using the united atom model to quantitatively study the effect of molecular orientation induced by extensional strains on the free volume distribution in polymers. We also investigated whether the increase in the number of larger, more elliptical free volume regions ("holes" or "cavities") with stretch is observable using our computational approach. To identify the regions where significant free volume changes are occurring, we used the Voronoi tessellation technique, which provides better identification tools for the location of free volume "cavities" with respect to identifiable monomers on the polymer chains. Since the distribution of free volume has more influence on many polymer properties than the total free volume,

10.1021/ma034758p CCC: $25.00
Published on Web 10/09/2003

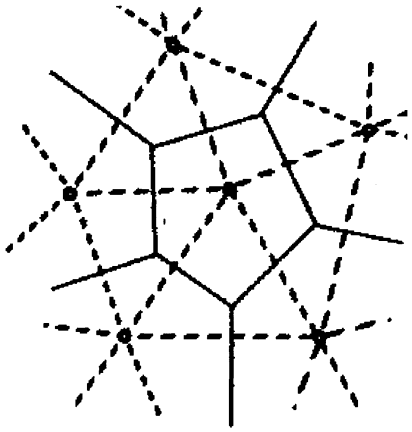

Figure 1. Two-dimensional representation of a Voronoi polygon. The network formed by the dashed lines is the result of the Delauney tessellation.

Voronoi tessellation provides us an effective way of identifying the distribution of the free volume.

Methodology

A domain-decomposition parallel MD code was used to evaluate the change in molecular architecture due to applied strains. In the domain decomposition method the physical domain is divided into subdomains, so that each processor only needs to account for a subdomain as a part of the whole system. This accelerates the simulation speed on parallel computers where more than one processor is available.[19,20]

A model linear polymer was used for this study. Even though the model resembles polyethylene, our objective was to understand the behavior of a simple semicrystalline polymer with essential attributes of polymer connectivity, constrained flexibility, and van der Waals interactions.[21] A united atom model was used, and the force field used to compute the forces on each unit in the united atom method is explained below. This force field was used previously and has provided realistic results.[21] The covalent bond between two atomic clusters is treated as a rigid bond where the bond length is always equal to 1.53 Å.

The following bond angle potential (Φ_θ) was used in our calculations:

$$\Phi_\theta = {}^1/_2 k_\theta(\cos\theta - \cos\theta_0)^2 \tag{2}$$

where k_θ is a constant for a bending spring that idealizes the bond angle variation, whose value is taken to be 520 kJ/mol, θ_0 is the equilibrium bond angle (112.813°), and θ is the bond angle at any time.

Torsional potential restricts molecular rotation around single bonds due to steric hindrance. In our program the torsional potential for a given dihedral angle is taken as

$$\Phi(\tau) = \sum_{m=0}^{5} C_m \cos^m \tau \tag{3}$$

where τ is the dihedral angle which varies from −180° to +180° with $\tau = 0°$ corresponding to the trans conformation. C_m are the coefficients of a polynomial. For the united atom model, the values of C_m are taken as 8832.1806, 18 087.0660, 4880.8037, −31 800.0510, 0, and 0 J/mol, respectively.

The Weeks−Chandler−Andersen (WCA) potential is used as nonbonded potential in order to account for the nonbonded interactions:

$$\Phi(|r_{ij}|) = 4\epsilon((\sigma/|r_{ij}|)^{12} - (\sigma/|r_{ij}|)^6) + \epsilon \quad \text{for} |r_{ij}| \le 2^{1/6}\sigma$$
$$= 0 \quad \text{for} |r_{ij}| > 2^{1/6}\sigma \tag{4}$$

where $\sigma = 4.28$ Å and $\epsilon = 57.0$ kJ/mol.

Columbic interactions were not included for our polymer as they are nonpolar molecules. Since MD simulations are computationally intensive, sample size should be small enough to be suitable for the current computational capabilities but large enough to capture the essential physics of the behavior we are trying to capture. Therefore, an adequate compromise between both requirements must be found. With current computational facility, the total number of particles in a sample cannot be more than several million. Generally, several hundreds to several tens of thousands of atoms or atom units are used in these types of simulations. Because the simulation cell is small compared to real systems, the periodic boundary condition (PBC) is used to reduce the influence of boundary effects on the simulation results. By applying PBC to simulations, artificial symmetry is introduced to the system. For crystalline material this technique is valid and improves the rigor and realism of molecular simulation results.

The loose coupling technique of Berendsen et al. is used to control the temperature during simulation.[22] The internally measured temperature, $T(t)$, is coupled to an external heat bath at a temperature $T_{\text{req}}(t)$ using the following relation:

$$\dot{T}(t) = \frac{-1}{\tau_T}(T(t) - T_{\text{req}}(t)) \tag{5}$$

where τ_T is user specified relaxation time that determines how fast the actual temperature approaches to the required value.

In addition to the temperature control, the pressure tensor should also be controlled. The size and shape of the simulation box change according to the following equation:

$$\dot{h}(t) = \frac{P(t) - P_{\text{req}}(t)}{\tau_p \mu} \tag{6}$$

where μ is a predefined constant and τ_p is a user-defined relaxation time, P is the internally measured pressure tensor, and P_{req} is the required pressure tensor. The loose coupling technique is naturally overdamped and produces smoother, less oscillatory response to sudden changes in pressure or temperature.

The simulations were done on a Silicon Graphics Origin2000 parallel system with 28 processors. First, a sample made of 400 C100 chains with a density of 0.7 g/cm^3 was prepared. It was generated by the Pivot Monte Carlo (Pivot MC) sampling technique at 300 K. It was shown that Pivot MC sampling prepared an initial distribution of chain configurations which is not only unbiased but also very close to that expected of the bulk melt.[23] Before a tensile stress is applied, the prepared sample was heated to 525 K at a rate of 0.1 K/ps. Then the sample was relaxed at that temperature for 3 ns. After that, it was cooled to 300 K at a rate of 0.1 K/ps. Finally, a tensile stress was applied at rate of

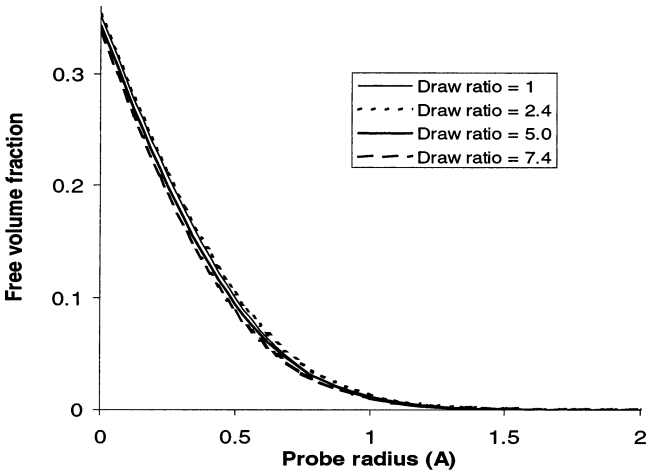

Figure 2. Free volume fractions accessible to spherical probes of different sizes.

1 bar/ps. PBC was applied for all simulations. The boundary deformation of polymer sample under the applied stress was used to calculate the draw ratio (the ratio of the final length of sample to its original length as known in textile science) to represent the amount of stretch.

The algorithm of Gerstein et al. was used to implement Voronoi tessellation[24,25] which uniquely and completely divides the system volume into polyhedra comprising the space nearest to each atom. The volume of each polyhedron can be calculated from the tessellation result, which was then used to study the evolution of free volume.

In the hard-sphere probe method, the periodic box is divided into small cubic subcells with the grid size equal to 0.4 Å. All of the atoms were assumed to be hard spheres with radii equal to 88% of the full van der Waals radii (R_{vdw}). If a small probe sphere of radius R_p is inserted into the system, then $R = R_{vdw} + R_p$ represents the radius of the volume that is excluded to the atom center. A subcell is considered to be occupied whenever more than half of the subcell size lay within any hard sphere of radius R.

Results and Discussion

Effect of Probe Radius on Free Volume Fraction. The amount of free volume depends on the size of the probe used for identifying and calculating the free volume. Figure 2 shows the dependence of free volume fraction on the probe radius R_p for a polymer sample for various strain levels. It can be seen that the free volume fraction is roughly equal to 35% for $R_p = 0$ when draw ratio is equal to one, which is close the simulation results for polybutadiene[8] (32%) and polycarbonate[26] (39%) for probe radius equal to 0. With increasing draw ratio, the total free volume is decreased. It is clear from the figure that the free volume fraction depends on the size of the probe, as the size increases free volume decreases rapidly. When the probe radius is above 1.5 Å, almost no free volume is accessible.

When the probe radius is less than 0.5 Å, voids with "infinite" size are found in the bulk system with periodic boundary conditions, as all cavities are interconnected when probed with a small probe. By increasing the probe size further, all of the free volume breaks up into discrete voids of finite size depending on the size of the probe. In this study, the "connectivity" between unoccupied regions was accomplished with a hard-sphere of radius 1 Å. This connectivity diminishes significantly with a larger probe size. When explored with a probe size of 1 Å, the free volume fraction was calculated to be around 1% for the system we studied. It is worthwhile to note that a comparable simulation result in the literature[9] for a PBO system with a probe radius of 1 Å was 0.61%. From Figure 2, one can see that the total free volume increases slightly for small uniaxial strains followed by a larger reduction for higher strains. The magnitude of changes in free volume induced by stretch is not that significant compared to choice of the probe size, and irrespective of the probe size, the free volume initially increases and then decrease with increasing axial strains. Even though the changes in the free volume due to stretch is not very high on an absolute scale, it should be noted that many properties, such as viscosity, change exponentially with the changing free volume fraction. Thus, small changes in free volume could result in significant changes in polymer properties. Some polymer properties, such as diffusion, depend not only on the total free volume but also on the orientation and shape of the regions that form the total free volume. In the following section we calculate the change of the shape of free volume "cavities" due to stretch.

Table 1. Distribution of Void Size at Different Draw Ratios (Unit Is number/nm^3)

	draw ratio			
void size (Å^3)	1	2.4	5.0	7.4
<5	75.816	65.608	56.869	53.294
5−10	2.404	2.438	2.150	1.755
10−20	1.435	1.833	1.440	1.318
20−40	0.491	0.834	0.710	0.685
40−60	0.032	0.197	0.200	0.150
60−100	0.000	0.064	0.072	0.072
≥100	0.000	0.000	0.006	0.013
total	80.178	70.974	61.446	57.287

Effect of Orientation on Free Volume Distribution. Free volume distribution was analyzed at three different draw ratios, namely 2.4, 5.0, and 7.4. The Herman's orientation function calculated from molecular configurations predicted from MD corresponding to these draw ratios are 0.49, 0.66, and 0.76, respectively. Table 1 shows the number of cavities with specific ranges of cavity size for a sample volume of 1 nm^3. As one can see with increasing orientation, the number of larger free volume holes increases, while the total number of voids decreases.

For example, for void size between 60 and 100 Å^3, before stretching the number of voids with this size is 0 per nm^3 of polymer sample, which increased to 0.064, 0.072, and 0.072/nm^3 with stretching. One can also see a similar trend for void size bigger than 100 Å^3. However, the number-average void size for draw ratio 1, 2.4, 5.0, and 7.4 is 1.81, 1.24, 1.12, and 1.13 Å^3, respectively, which shows that the number-average void size is decreasing with the draw ratio rather rapidly at the initial stages of stretch and then seems to stabilize with further stretch. For intermediate sized cavities (5−20 Å^3) the number of voids initially increases and then decreases. The number of smaller cavities decreases with stretch while the number of larger cavities (of size above 40 Å^3) in general increases.

To understand the effect of stretch on the shape of cavities, the shape factor w was analyzed for various draw ratios, and the results are shown in Table 2. A

Table 2. Shape Factor *w* for Voids with Different Size Range at Different Draw Ratios

	draw ratio			
void size (Å^3)	1	2.4	5.0	7.4
<5	1.38	1.37	1.38	1.38
5−10	2.42	2.41	2.41	2.42
10−20	2.65	2.61	2.58	2.58
20−40	2.89	2.82	2.79	2.79
40−60	3.54	3.10	2.98	3.11
60−100	N/A	3.55	3.28	3.13
≥100	N/A	0	3.60	4.10

larger value in shape factor suggests the void or cavity is elongated. From Table 2 several observations can be made. At any given strain, increasing cavity size is associated with increasing shape factor, indicating that larger voids are more elliptical than smaller ones and the shape factor increases with the size of the cavity. Also, one can observe that with increasing orientation more elongated lager voids are formed in the sample corresponding to the largest size of voids. For example, when the draw ratio is 7.4, the shape factor corresponding to voids with volume greater than 100 Å^3 is 4.10 whereas there were no voids with the size greater than 100 Å^3 before stretching. Also, the shapes of very small cavities (up to 5 Å^3) are generally unchanged due to elongational strains, while the intermediate size cavities (10−100 Å^3) becomes more spherical during the stretch due to the breakup of cavities to smaller ones or simply due to the change in their shape. For the voids larger than 100 Å^3, considering the size distributions due to stretch obtained from Table 1, these results indicate that the larger cavities with increased shape factor is the result of coalescing smaller cavities to form larger ones.

Mechanism for the Formation of Large Voids with Stretching. As the polymer is stretched, the polymer chains tend to align for better packing, resulting in the reduction of total free volume. However, both experimental and simulation data show the that number of larger, more elongated free volume regions increases with increasing orientation. So far, there are no explanations from experimental observations. It is logical to assume that the free volume cavities around a chain end are more likely to increase when the polymer sample is subjected to an applied tensile force, since atoms can be pulled apart more easily at these locations. To verify this assumption, a Voronoi tessellation technique was applied to study the polyhedron volume distribution of our system.

Using Voronoi tessellation, the free volume distribution associated with atoms positioned at the ends of polymer chains can be separated from those associated with other atoms. Figure 3 shows the simulation results indicating the distribution of relative free volume associated with atoms located at the ends of polymer chains and corresponding Voronoi polygon size (with *y* axis showing the ratio of the number of atoms or atomic units with a specific polyhedron volume to the total number of atomic units in the system). Voronoi polygons are created surrounding each atom such that the unoccupied regions between atoms are shared between polygons associated with neighboring atoms. As the polymer undergoes stretch, the Voronoi polygons are redrawn with respect to the new atomic positions. From Figure 3 one can see that the polyhedron volume increases with increasing draw ratio, indicating the free volume region around chain ends increases with increasing orientation. The average polyhedron volume for draw ratio 1, 2.4, 5.0, and 7.4 are 52.56, 55.70, 55.71, and 55.83 Å^3, respectively. On the other hand, with increasing draw ratio one can see decreasing polyhedron volume associated with atoms away from the ends of the polymer chains (Figure 4). The average polyhedron volume for draw ratio 1, 2.4, 5.0, and 7.4 are 31.74, 31.88, 31.55, and 31.36 Å^3, respectively. One can notice that when draw ratio is 2.4, the average polyhedron volume increases slightly, which was also observed by Shelby et al.[18] This expansion is possibly due to the Poisson effect. As the draw ratio is increased, however, the chains begin to pack better and the resulting densification starts to dominate. As one can see, the distribution in Figure 4 shifts toward the left with increasing stretch, while the overall distribution shifts toward the right in Figure 3.

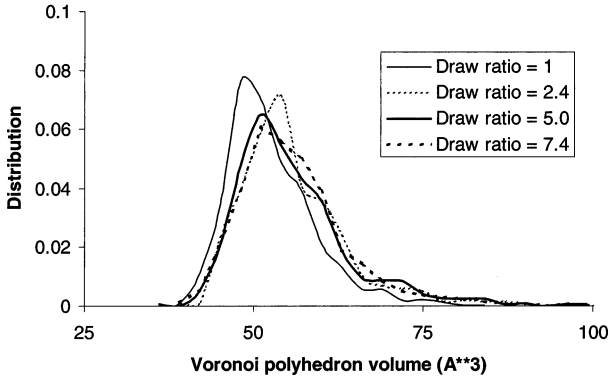

Figure 3. Voronoi polyhedra volume distribution for atoms at chain ends.

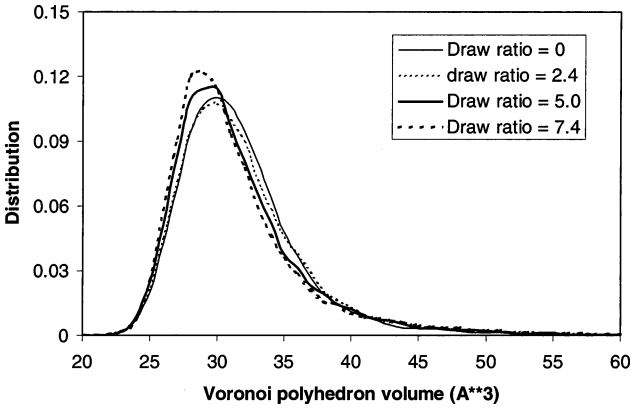

Figure 4. Voronoi polyhedra volume distribution for atoms located away from chain ends.

Conclusion

In this work we studied the effect of stretch and resulting molecular orientation on the free volume distribution in a model polymer using a united atom molecular dynamics approach. The hard-sphere probe analysis shows free volume fraction decreases dramatically with increasing probe radius. When probe radius is equal to 0, the free volume fraction is around 35%. When the probe radius is larger than 1.5 Å, the free volume fraction is almost zero. In this study the "connectivity" for distributed free volume cavities was accomplished with a hard sphere of radius 1 Å, which is comparable to the radius of orthopositronium that is used to investigate the free volume in PAL technique. With the introduction of this probe, the free volume fraction is around 1% in an unstrained isotropic sample.

The simulation results confirmed the experimental observation that chain alignment causes an increase in the number of larger, more elliptical free volume cavities in polymers, while the effective density increases associated with a decrease in the total free volume due to increasing extensional strains. Moreover, the simulation results provided a more quantitative picture of the evolution of the distribution of free volume in the system as well as the evolution of the shape of the "cavities" that constitute the free volume.

The Voronoi polyhedron volume distribution for atoms at the polymer chain ends shows increasing free volume with stretch, while the polyhedron volume distribution for atoms not at chain ends shows decreasing volume with increasing extensional strains. This phenomenon indicates that the larger voids associated with the free volume during stretching is formed at chain ends.

The exact definition of free volume is somewhat ambiguous and is often defined in subtly different way for a particular phenomenon.[4] It should be noted that the Voronoi polyhedron volume only gives a measure of the free volume associated with that particular atomic unit, and in order to get the free volume from these data, one has to filter out the hard-sphere van der Waals volume of the atomic unit from the polyhedron volume by assuming appropriate temperature-dependent van der Waals radius to account for the mobility from vibrational amplitudes.[4] These difficult choices are not incorporated in this paper since using Voronoi tessellation method we are investigating only the location of significant changes in free volume.

Acknowledgment. This work was sponsored by the National Textile Center and the US Department of Commerce under Grants 2706B48 and 2706M57. We thank Dr. David Brown and Dr. Mark Gerstein for providing us computer codes used in this work. We thank Dr. Sergei Nazarenko for discussions related to PALS.

References and Notes

(1) Wang, B.; Wang, Z. F.; Zhang, M.; Liu, W. H.; Wang, S. J. *Macromolecules* **2002**, *35*, 3993.
(2) Haraya, K.; Hwang, S. T. *J. Membr. Sci.* **1992**, *71*, 13.
(3) Kobayashi, Y.; Haraya, K.; Hattori, S.; Sasuga, T. *Polymer* **1994**, *35*, 925.
(4) Rigby, D.; Roe, R. J. *Macromolecules* **1990**, *23*, 5312.
(5) Kobayashi, Y.; Zheng, W.; Mwyer, E. F.; McGervey, J. D.; Jamieson, A. M.; Simha, R. *Macromolecules* **1989**, *22*, 2302.
(6) Yu, W. C.; Sung, C. S. P.; Robertson, R. E. *Macromolecules* **1988**, *21*, 355.
(7) Victor, J. G.; Torkelson, J. M. *Macromolecules* **1988**, *21*, 3490.
(8) Misra, S.; Mattice, W. L. *Macromolecules* **1993**, *26*, 7274.
(9) Kim, W.; Mattice, W. L. *Comput. Theor. Polym. Sci.* **1998**, *8*, 353.
(10) Voorintholt, R.; Kosters, M. T.; Vegter, G.; Vriend, G.; Hol, W. G. J. *J. Mol. Graphics* **1989**, *7*, 243.
(11) Sastry, S.; Corti, D. S.; Debenedetti, P. G.; Stillinger, F. H. *Phys. Rev. E* **1997**, *56*, 5524.
(12) Sastry, S.; Truskett, T. M.; Debenedetti, P. G.; Torquato, S.; Stillinger, F. H. *Mol. Phys.* **1998**, *95*, 289.
(13) Tanemura, M.; Ogawa, T.; Ogita, N. *J. Comput. Phys.* **1983**, *51*, 191.
(14) Vittoria, V.; De Candia, F.; Capodanno, V. *J. Polym. Sci., Part B: Polym. Phys.* **1986**, *24*, 1009.
(15) Williams, J. L.; Peterlin, A. *J. Polym. Sci., Part B: Polym. Phys.* **1971**, *9*, 1483.
(16) DE Candia, F.; Perullo, A.; Vittoria, V.; Peterlin, A. *J. Appl. Polym. Sci.* **1983**, *28*, 1815.
(17) Shelby, M. D.; Hill, A. J.; Burgar, M. I.; Wilkes, G. L. *J. Polym. Sci., Part B: Polym. Phys.* **2001**, *39*, 32.
(18) Shelby, M. D.; Wilkes, G. L. *Polymer* **1998**, *39*, 676.
(19) Brown, D.; Clarke, J. H. R.; Okuda, M.; Yamazaki, T. *Comput. Phys. Commun.* **1994**, *83*, 1.
(20) Plimpton, S. J.; Hendrickson, B. A. *Mater. Res. Soc. Symp. Proc.* **1993**, *291*, 37.
(21) Brown, D.; Clarke, J. H. R. *Macromolecules* **1991**, *24*, 2075.
(22) Berendsen, H. J. C.; Postma, J. P. M.; van Gunsteren, W. F.; DiNola, A.; Haak, J. R. *J. Chem. Phys.* **1984**, *81*, 3684.
(23) Brown, D.; Clarke, J. H. R. *J. Chem. Phys.* **1994**, *100*, 6011.
(24) Gerstein, M.; Tsai, J.; Levitt, M. *J. Mol. Biol.* **1995**, *249*, 955.
(25) Harpaz, Y.; Gerstein, M.; Chothia, C. *Structure* **1994**, *2*, 641.
(26) Arizzi, S.; Mott, P. H.; Suter, U. W. *J. Polym. Sci., Part B: Polym. Phys.* **1992**, *30*, 415.

MA034758P